

## SUPPORTING INFORMATION

Manuscript title: **Allosteric binding properties of a 1,3-*alternate* thiocalix[4]arene-based receptor having phenylthiourea and 2-pyridylmethyl moieties on opposite faces**

Author(s): Shofiur Rahman,<sup>a,c</sup> Hirotsugu Tomiyasu,<sup>a</sup> Chuan-Zeng Wang,<sup>a,b</sup> Paris E. Georghiou,<sup>c\*</sup> Abdullah Alodhayb,<sup>d</sup> Cameron L. Carpenter-Warren,<sup>e</sup> Mark R. J. Elsegood,<sup>e</sup> Simon J. Teat,<sup>f</sup> Carl Redshaw,<sup>g</sup> and Takehiko Yamato<sup>a\*</sup>

<sup>a</sup> Department of Applied Chemistry, Faculty of Science and Engineering, Saga University, Honjo-machi 1, Saga 840-8502 Japan, E-mail: [yamatot@cc.saga-u.ac.jp](mailto:yamatot@cc.saga-u.ac.jp)

<sup>b</sup> School of Chemical Engineering, Shandong University of Technology, Zibo 255049, P. R. China

<sup>c</sup> Department of Chemistry, Memorial University of Newfoundland St. John's, Newfoundland and Labrador A1B 3X7, Canada; E-mail: [parisg@mun.ca](mailto:parisg@mun.ca)

<sup>d</sup> Department of Physics and Astronomy, College of Science, King Saud University, Riyadh 11451, Saudi Arabia

<sup>e</sup> Chemistry Department, Loughborough University, Loughborough, LE11 3TU, UK

<sup>f</sup> ALS, Berkeley Lab, 1 Cyclotron Road, Berkeley, CA 94720, USA

<sup>g</sup> Department of Chemistry, The University of Hull, Cottingham Road, Hull, Yorkshire, HU6 7RX, UK

## Table of Contents (S1 to S18 are the page numbers)

S1~S2 – Title, authors and description of supporting information content

S3~S8 –  $^1\text{H}$  NMR and  $^{13}\text{C}$  NMR spectra of all compounds **2**, **3**, **4** and **5a–5c** (Figs. S1~S12)

S9~S11 – X-ray crystal structures of receptor **5a** (Figs. S13~S17)

S11 – Scheme S1. Schematic representation of possible mechanism of the formation of **6** from **5a**.

S12 – Fig. S18.  $^1\text{H}$  NMR spectroscopic stack plot of a  $\text{CDCl}_3$ – $\text{DMSO-}d_6$  (10:1, v/v) solution of **5b** ( $4.0 \times 10^{-3}$  M) upon addition of TBAF in  $\text{CD}_3\text{CN}$ . ( $K_a = 477 \pm 14 \text{ M}^{-1}$ ) and the screen capture from the 1:1 global fit analysis using <http://supramolecular.org>.

S13 – Fig. S19.  $^1\text{H}$  NMR spectroscopic stack plot of a  $\text{CDCl}_3$ – $\text{DMSO-}d_6$  (10:1, v/v) solution of **5a** ( $4.0 \times 10^{-3}$  M) upon addition of TBAF in  $\text{CD}_3\text{CN}$ . ( $K_a = 250 \pm 14 \text{ M}^{-1}$ ). and the screen capture from the 1:1 global fit analysis using <http://supramolecular.org>.

S14 – Fig. S20.  $^1\text{H}$  NMR spectroscopic stack plot of a  $\text{CDCl}_3$ – $\text{DMSO-}d_6$  (10:1, v/v) solution of **5c** ( $4.0 \times 10^{-3}$  M) upon addition of TBAF in  $\text{CD}_3\text{CN}$ .

Fig. S21. *Left*: UV–vis absorption spectra changes of **5c** ( $2.5 \mu\text{M}$ ) upon the addition of  $\text{AcO}^-$  ion ( $0$ – $50 \mu\text{M}$ ) as its tetrabutylammonium salt in  $\text{CH}_2\text{Cl}_2$ – $\text{DMSO}$  (10:1, v/v) at 298 K. *Right*: Job plot showing the 1:1 binding of **5c** to  $\text{AcO}^-$  ion from the UV-vis titration method at 358 nm in  $\text{CH}_2\text{Cl}_2$ – $\text{DMSO}$  (10:1, v/v).

S15 – Fig. S22. *Left*: UV–vis absorption spectra changes of **5b** ( $2.5 \mu\text{M}$ ) upon the addition of  $\text{F}^-$  ion ( $0$ – $50 \mu\text{M}$ ) at 298 K as a TBAF salt in  $\text{CH}_2\text{Cl}_2$ – $\text{DMSO}$  (10:1, v/v). *Right*: Job plot showing the 1:1 binding of **5b** to  $\text{F}^-$  ion from the UV-vis titration method at 358 nm in  $\text{CH}_2\text{Cl}_2$ – $\text{DMSO}$  (10:1, v/v).

Table S1. The DFT interaction energies  $\Delta\text{IE}$  ( $\text{kJ mol}^{-1}$ ) calculated from the geometry optimized structure of receptor **L** (**5a**:  $\text{R} = \text{H}$ ; **5b**:  $\text{R} = \text{F}$ ; and **5c**:  $\text{R} = \text{NO}_2$ ) and complexes with the anions ( $\text{F}^-$ ,  $\text{Cl}^-$ ,  $\text{AcO}^-$ , and  $\text{H}_2\text{PO}_4^-$ ) and cation  $\text{Ag}^+$  by using B3LYP/LANL2DZ basis set in gas phase, dichloromethane (DCM) and dimethyl sulfoxide (DMSO) solvent system.

S16 – Fig. S23. Geometry-optimized structures of receptor of receptor **5a** ( $\text{R} = \text{H}$ ) and complexes with the anions and  $\text{Ag}^+$  ion by using B3LYP/LANL2DZ basis set in gas phase.

S17 – Fig. S24. Geometry-optimized structures of receptor of receptor **5b** and complexes with the anions and  $\text{Ag}^+$  ion in gas phase.

S18 – Fig. S25. Geometry-optimized structures of receptor of receptor **5c** and complexes with the anions and  $\text{Ag}^+$  by using B3LYP/LANL2DZ basis set in gas phase.

S18 – References

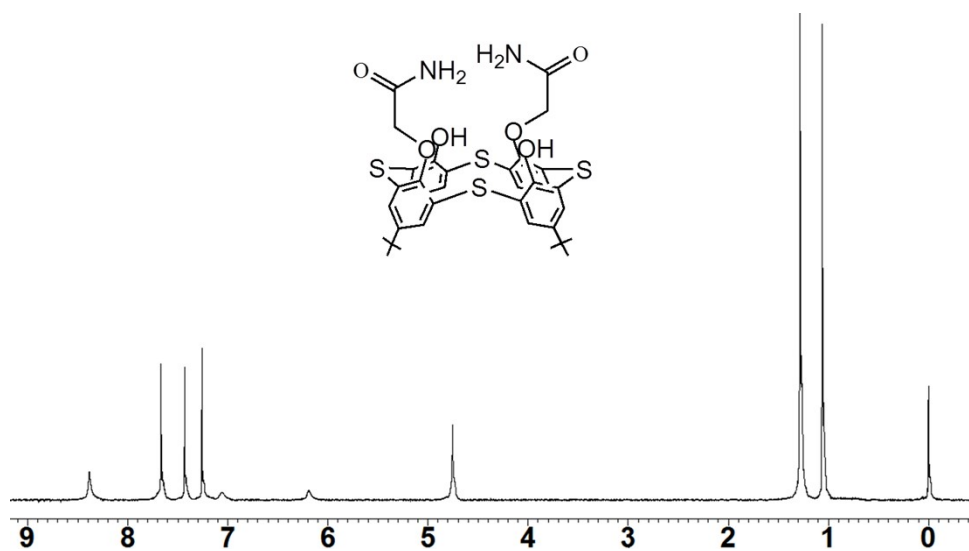


**Figure S1.**  $^1\text{H-NMR}$  spectrum of **2** (300 MHz,  $\text{CDCl}_3$ , 293 K).

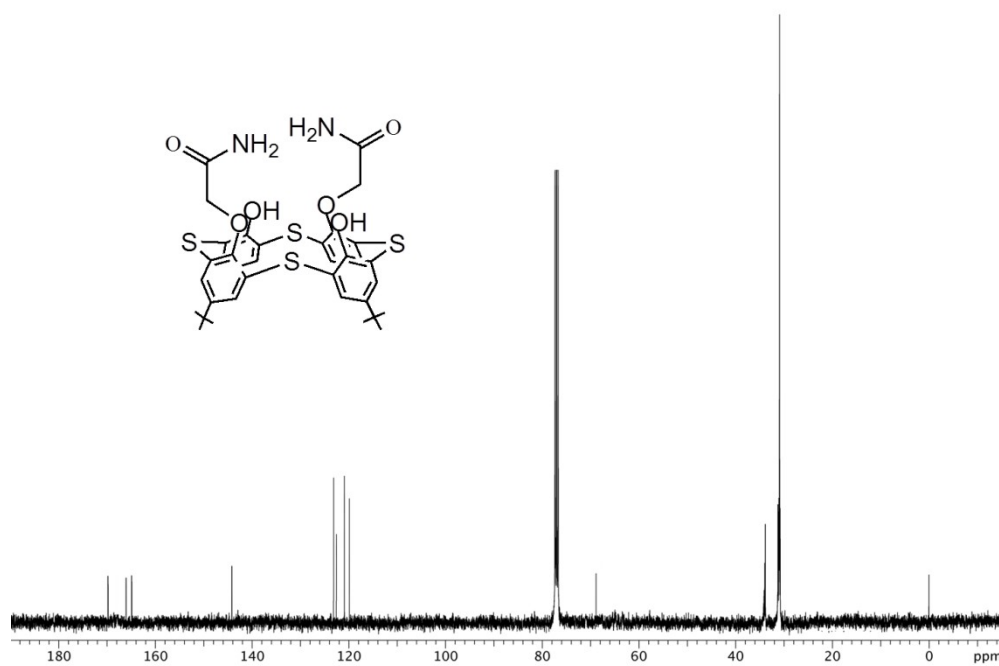


**Figure S2.**  $^{13}\text{C-NMR}$  spectrum of **2** (100 MHz,  $\text{CDCl}_3$ , 293 K).

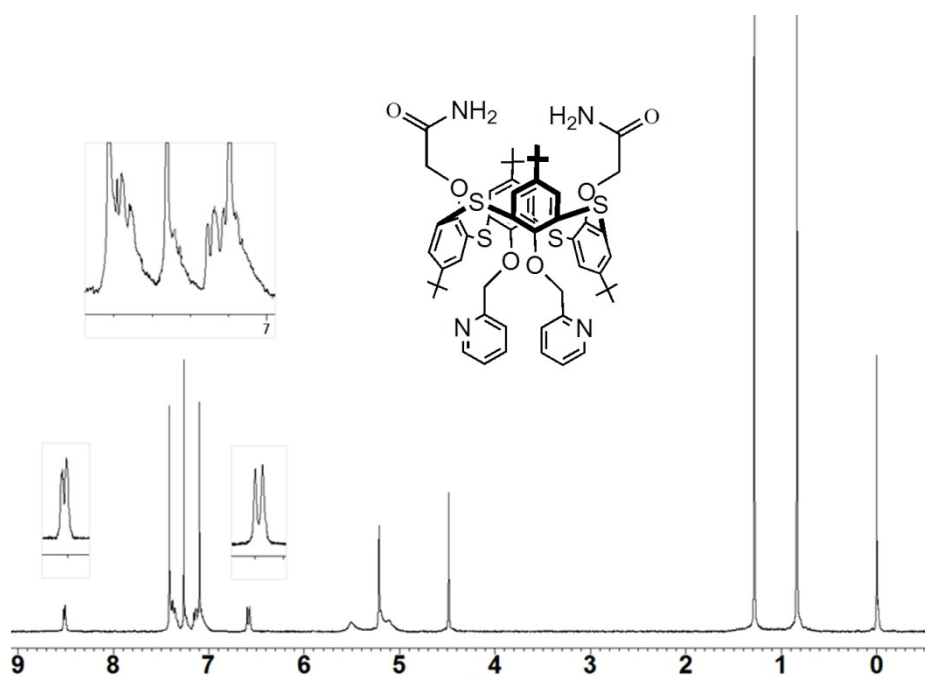


**Figure S3.**  $^1\text{H}$ -NMR spectrum of **3** (300 MHz,  $\text{CDCl}_3$ , 293 K).

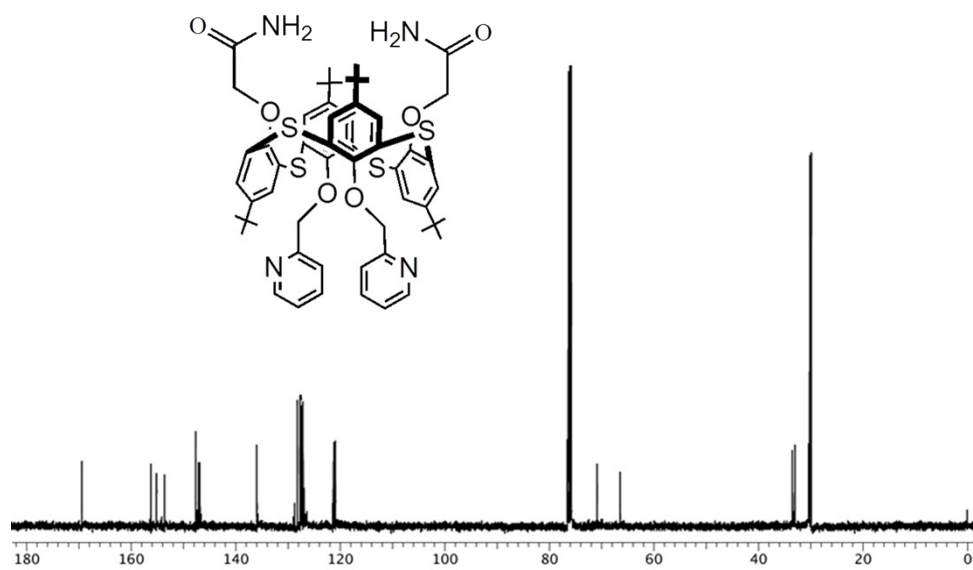


**Figure S4.**  $^{13}\text{C}$ -NMR spectrum of **3** (100 MHz,  $\text{CDCl}_3$ , 293 K).

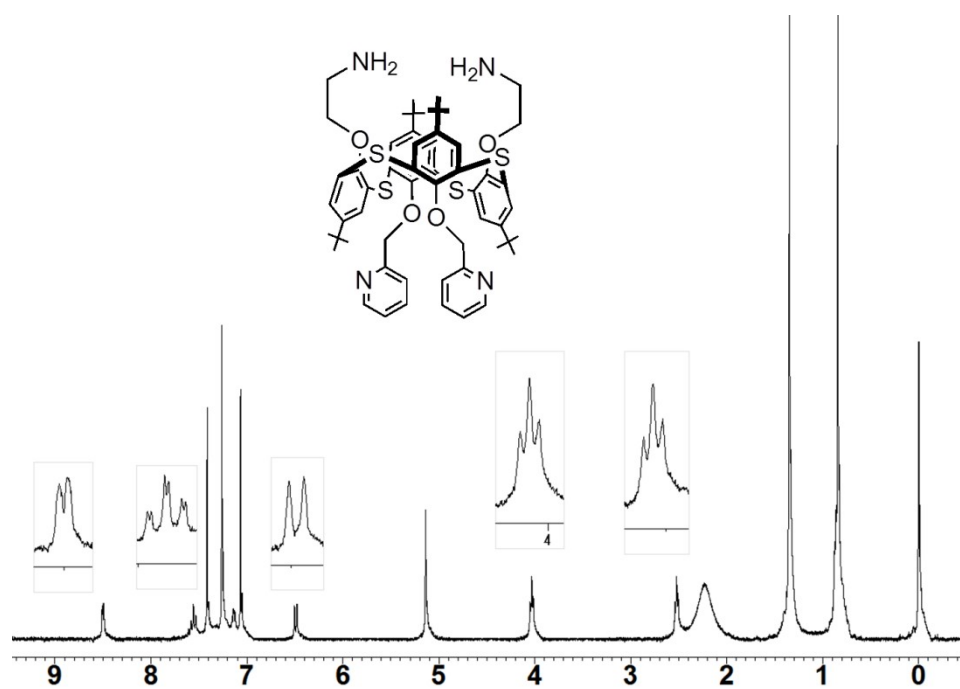


**Figure S5.**  $^1\text{H}$ -NMR spectrum of **4** (300 MHz,  $\text{CDCl}_3$ , 293 K).

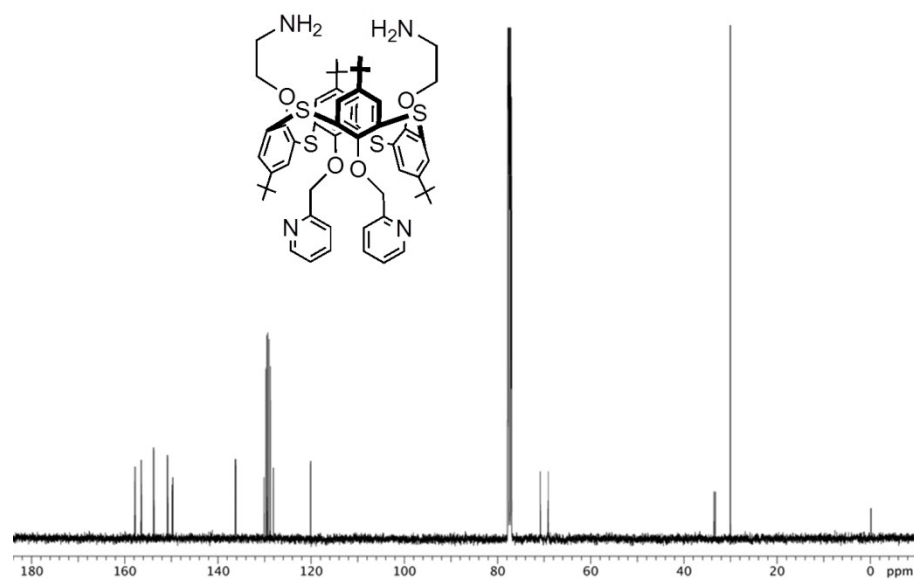


**Figure S6.**  $^{13}\text{C}$ -NMR spectrum of **4** (100 MHz,  $\text{CDCl}_3$ , 293 K).

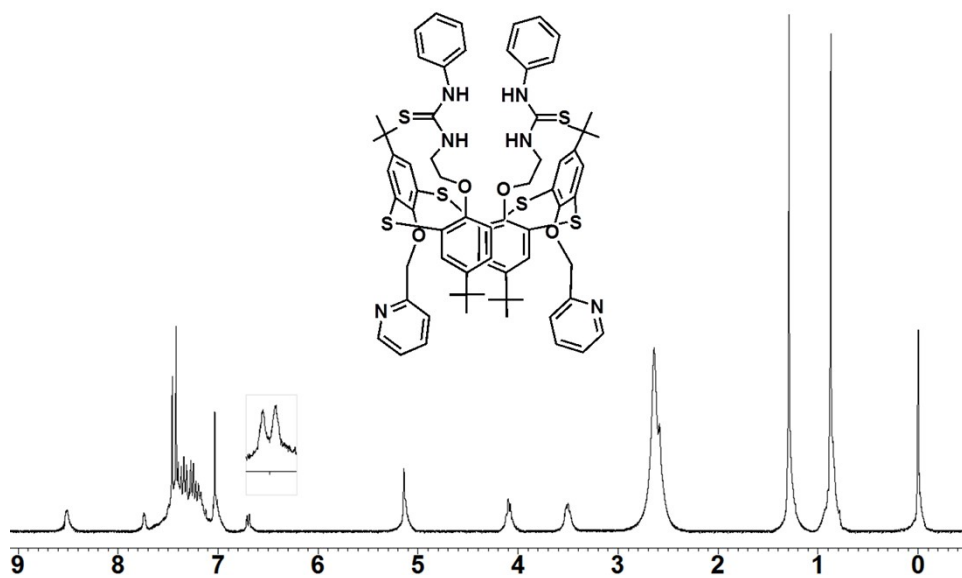


Figure S7.  $^1\text{H}$ -NMR spectrum of **5a** (300 MHz,  $\text{CDCl}_3$ , 293 K).

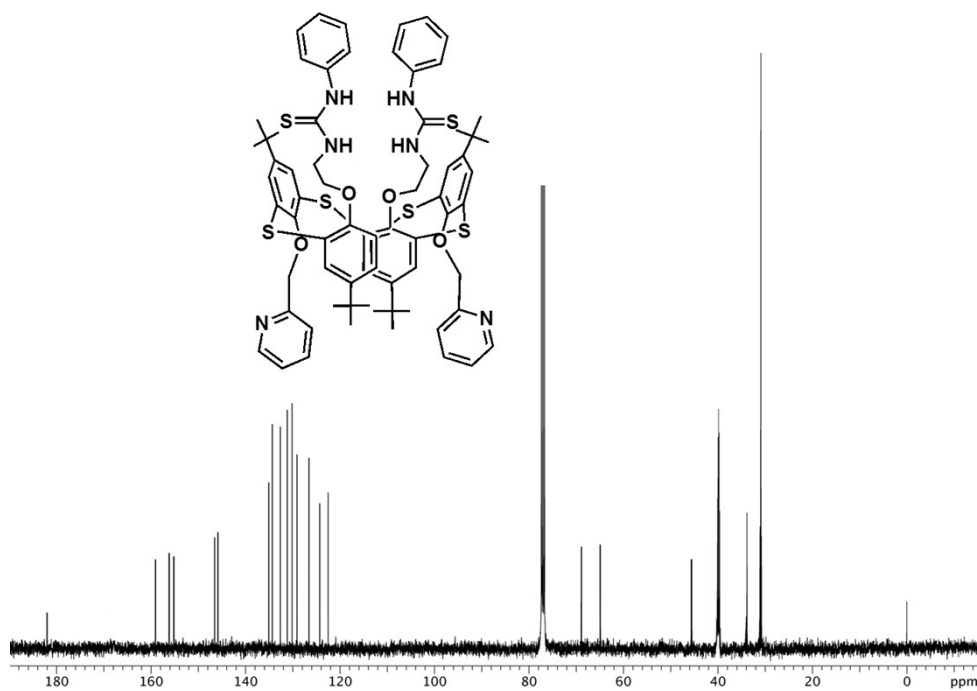
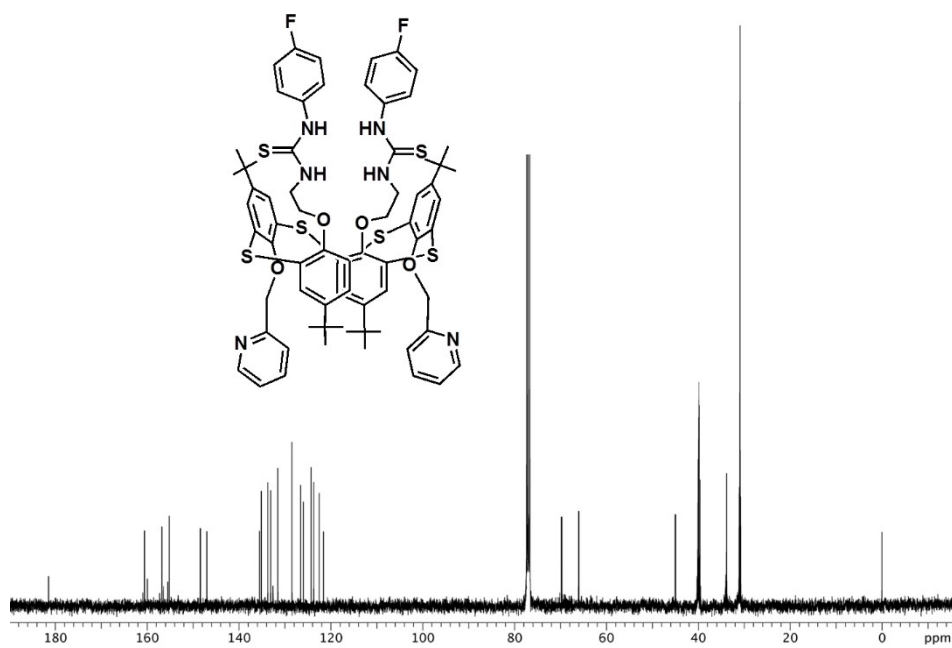
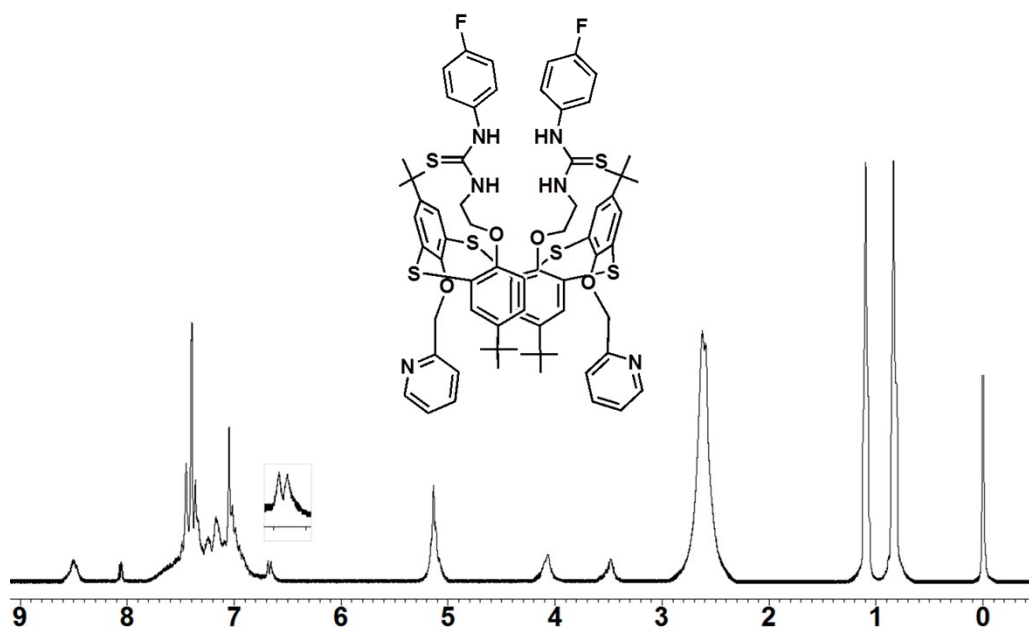


Figure S8.  $^{13}\text{C}$ -NMR spectrum of **5a** (100 MHz,  $\text{CDCl}_3$ - $\text{DMSO-}d_6$ , 293 K).



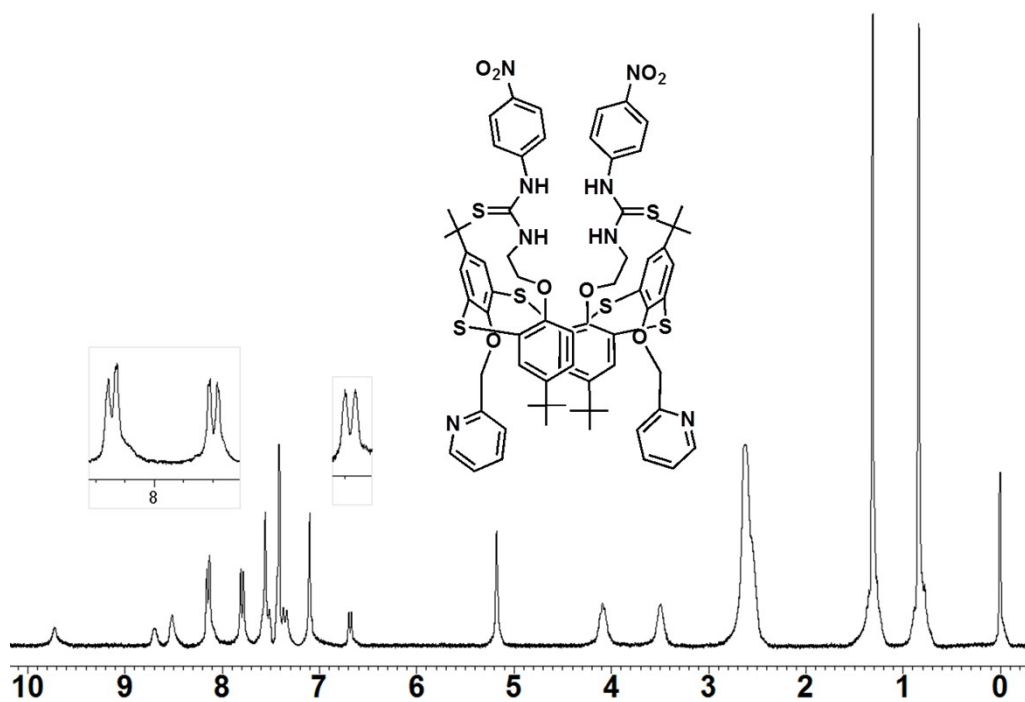


Figure S11.  $^1\text{H}$ -NMR spectrum of **5c** (300 MHz,  $\text{CDCl}_3$ - $\text{DMSO-}d_6$ , 293 K).

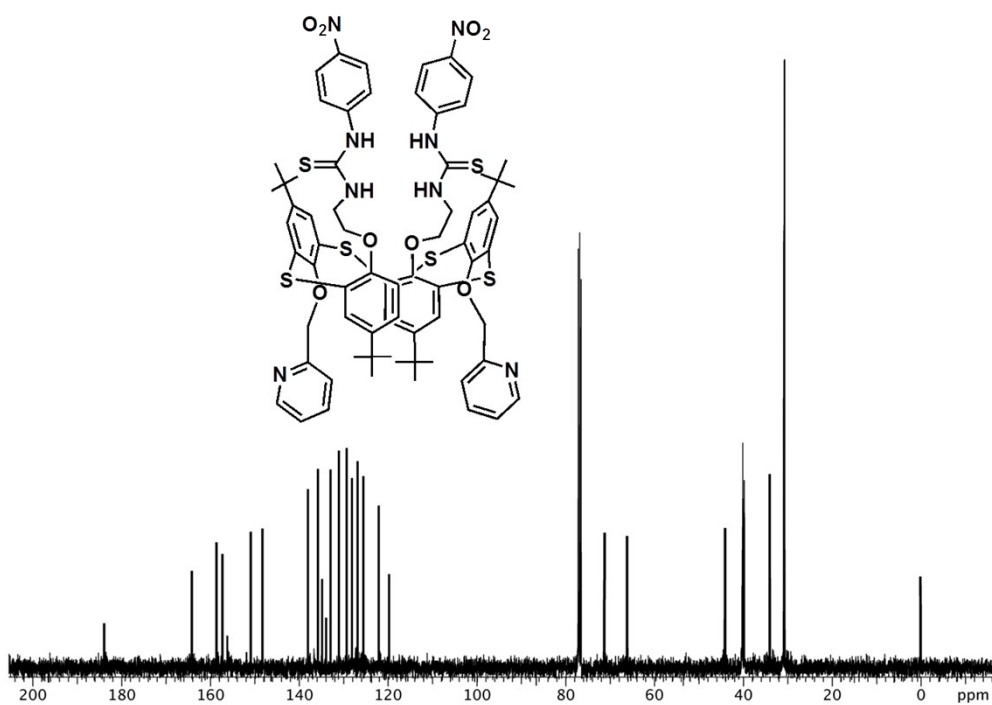
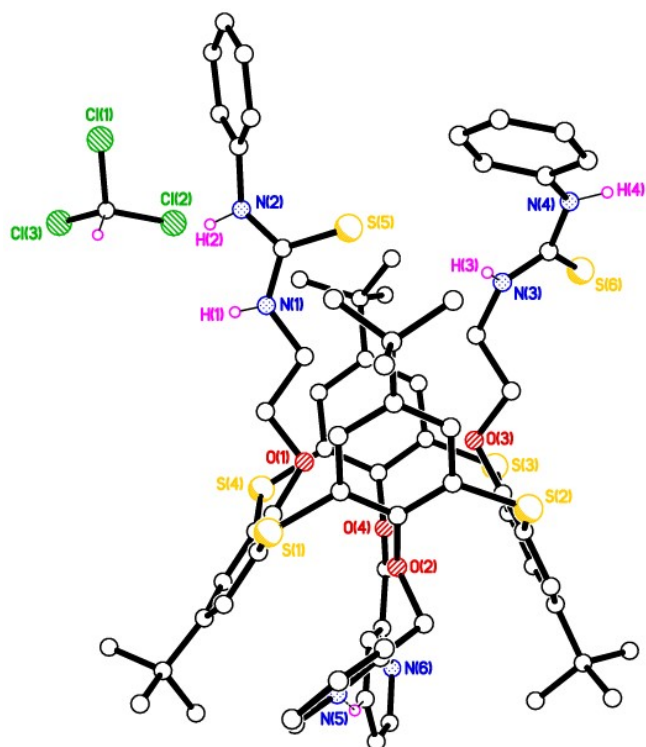


Figure S12.  $^{13}\text{C}$ -NMR spectrum of **5c** (100 MHz,  $\text{CDCl}_3$ - $\text{DMSO-}d_6$ , 293 K).



### X-ray crystal structure of receptor 5a



**Figure S13.** The first thiacalixarene in the asymmetric unit with the chloroform solvent of crystallization, showing intramolecular C–H···N hydrogen bonding between opposing pyridine rings. Minor disorder components and H atoms not involved in H-bonding are omitted for clarity.

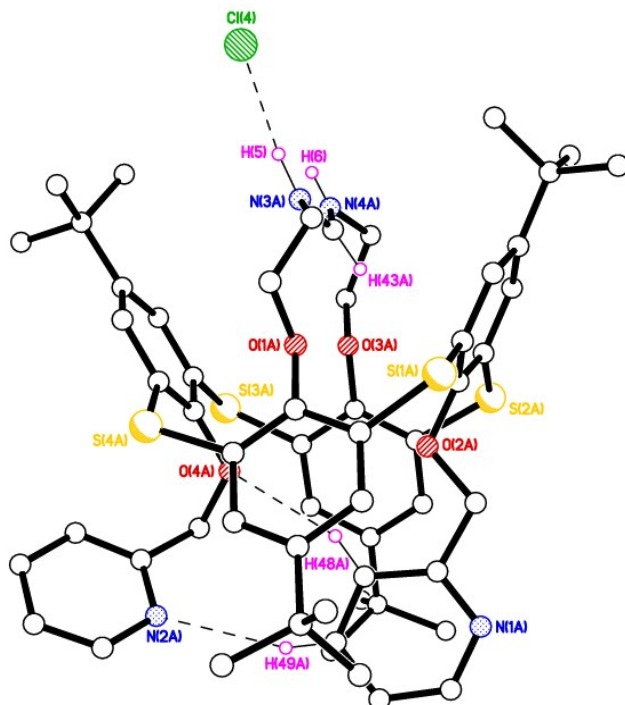


**Figure S14.** The second, modified, thiacalixarene in the asymmetric unit, showing intramolecular hydrogen bonding between opposing pyridine groups and the charge-assisted N–H<sup>+</sup>···Cl<sup>-</sup> hydrogen bonding at the top of the figure. Most H atoms not involved in H-bonding are omitted for clarity.

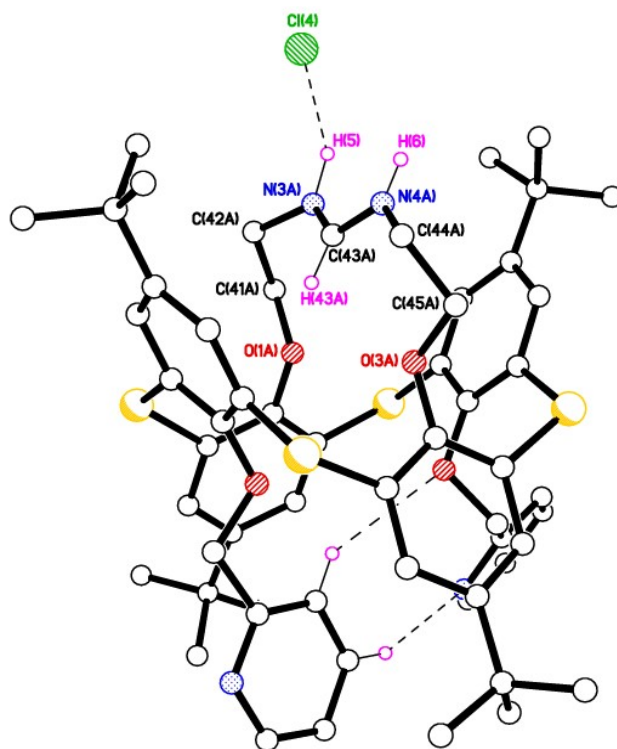


**Figure S15.** Alternative view of the second thiacalixarene in the asymmetric unit, emphasizing the novel functional group at the top of the molecule exhibiting a delocalized positive charge, acting as a counter cation for  $\text{Cl}^-$  anion capture. H atoms not involved in H-bonding are omitted for clarity.

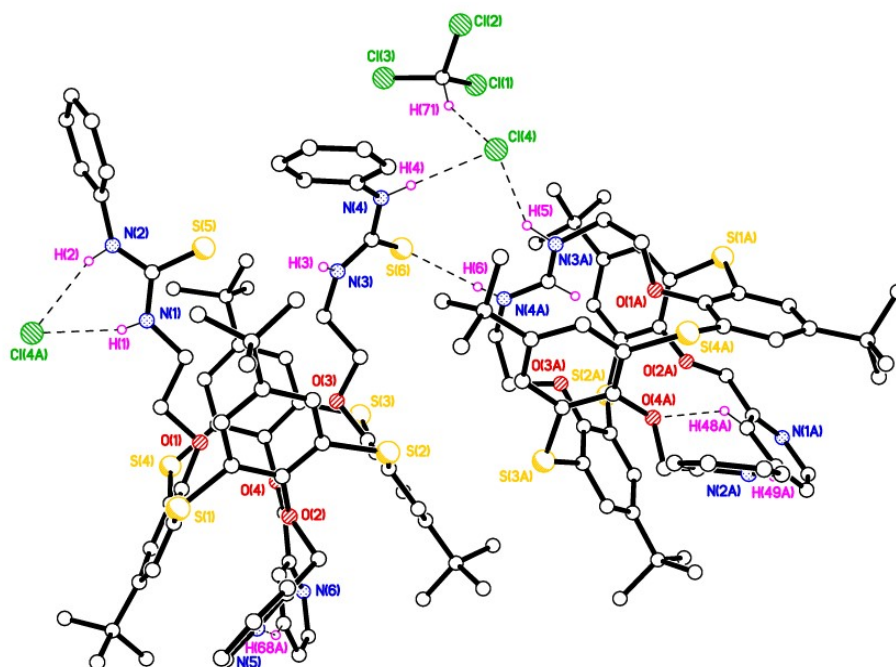


**Figure S16.** The asymmetric unit of **5a**, showing the intermolecular  $\text{S}\cdots\text{H}-\text{N}$  hydrogen bonding between the two thiacalixarenes and the  $\text{N}-\text{H}\cdots\text{Cl}$  interactions between each thiacalixarene and the  $\text{Cl}^-$  anion. Minor disorder components and H atoms not involved in H-bonding are omitted for clarity.

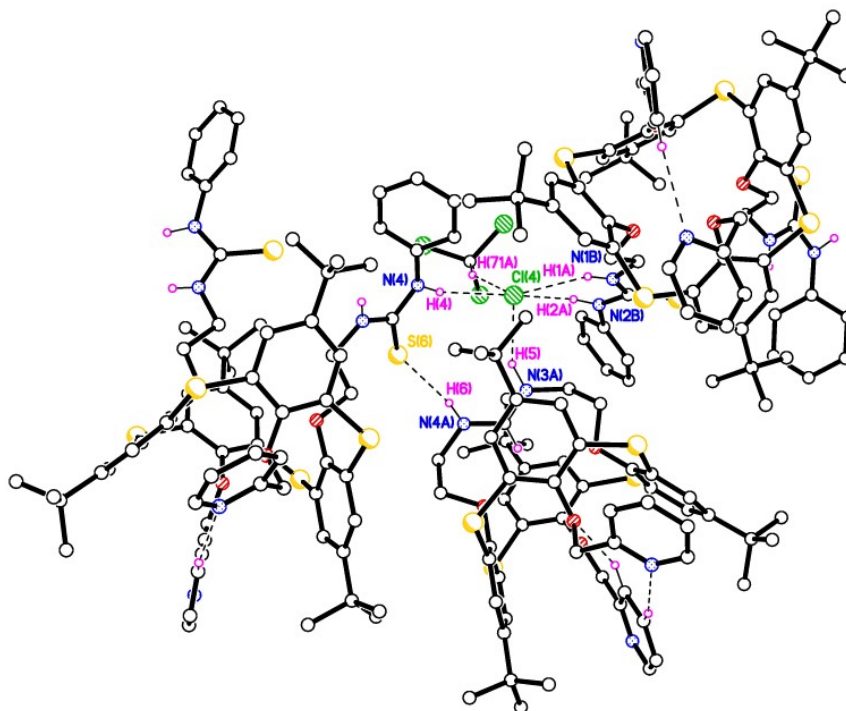
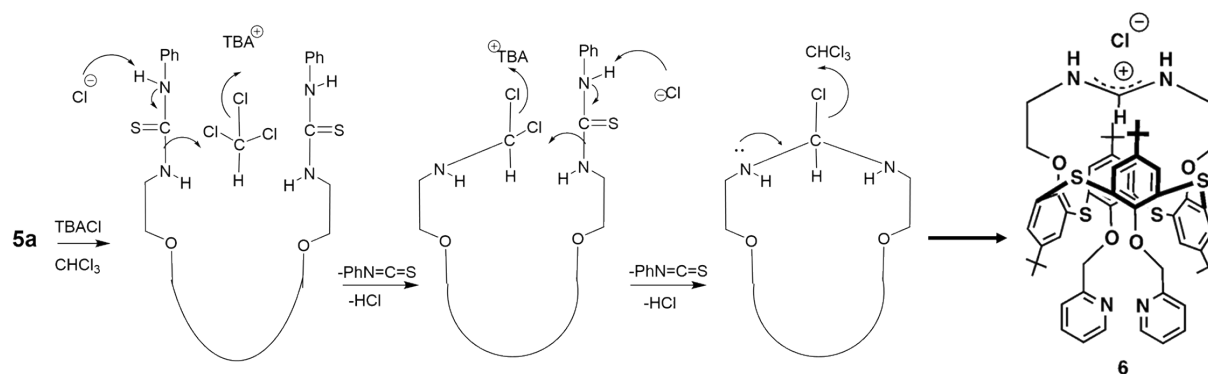
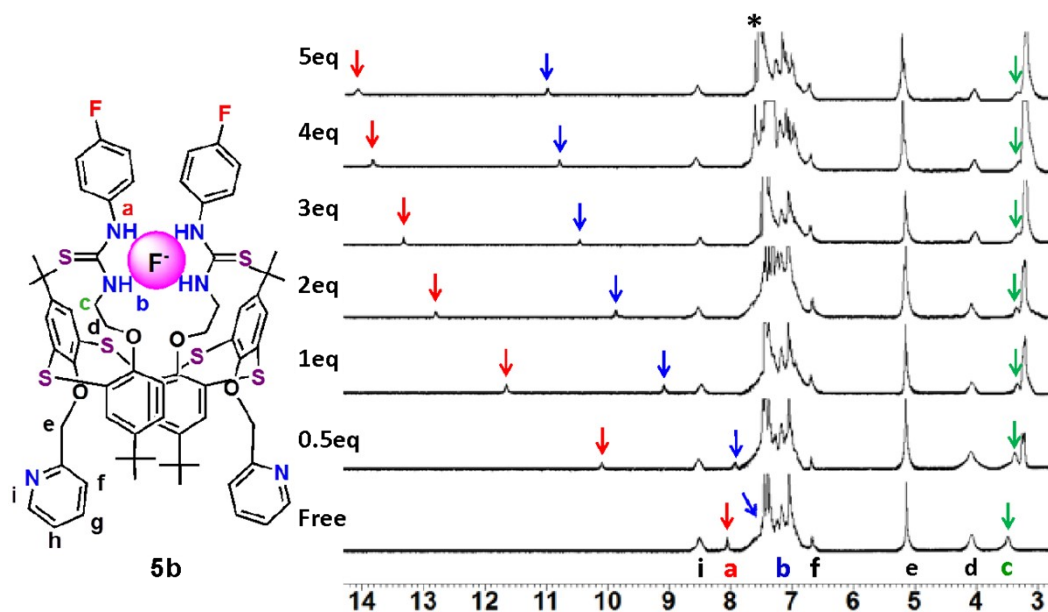


**Figure S17.** X-Ray crystal structure of **5a**, highlighting the capture of the  $\text{Cl}^-$  anion between three thiacalixarenes via  $\text{N-H}\cdots\text{Cl}$  hydrogen bonding and the (disordered) chloroform solvent of crystallization. Minor disorder components and H atoms not involved in H-bonding are omitted for clarity.



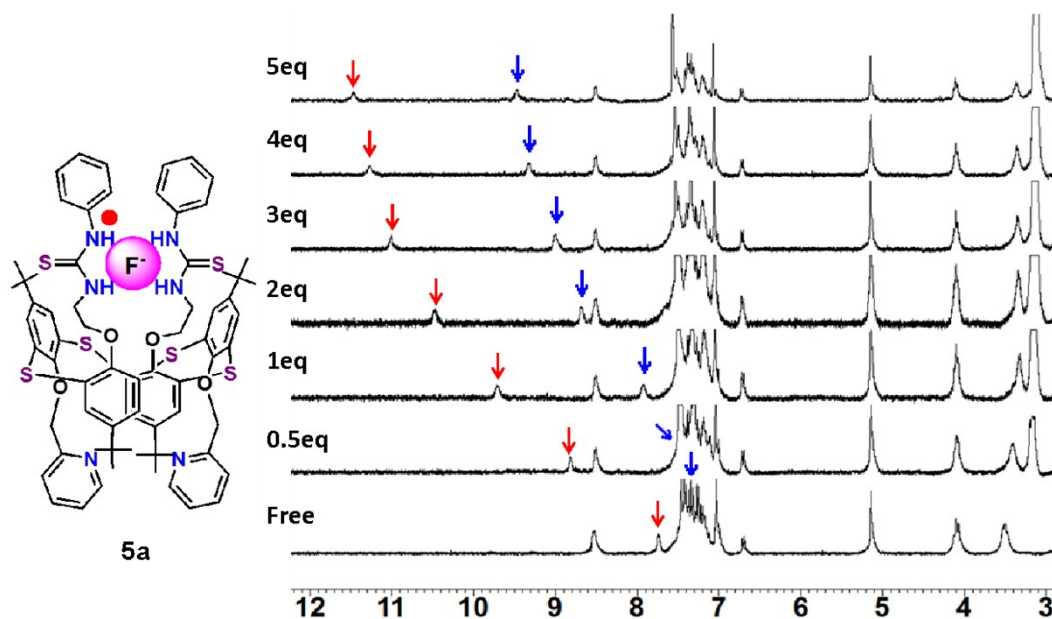
**Scheme S1.** Schematic representation of possible mechanism of the formation of **6** from **5a** in the presence of TBACl in  $\text{CHCl}_3$ .



| 5a (mol <sup>-1</sup> ) | F <sup>-</sup> (mol <sup>-1</sup> ) | NH <sub>a</sub> Proton (ppm) | NH <sub>b</sub> Proton (ppm) |
|-------------------------|-------------------------------------|------------------------------|------------------------------|
| 4.00E-03                | 0                                   | 8.050                        | 7.600                        |
| 4.00E-03                | 2.00E-03                            | 10.090                       | 8.420                        |
| 4.00E-03                | 4.00E-03                            | 11.550                       | 9.100                        |
| 4.00E-03                | 8.00E-03                            | 12.750                       | 9.820                        |
| 4.00E-03                | 1.20E-02                            | 13.300                       | 10.415                       |
| 4.00E-03                | 1.60E-02                            | 13.800                       | 10.750                       |
| 4.00E-03                | 2.00E-02                            | 13.850                       | 10.810                       |



**Figure S18.** <sup>1</sup>H NMR spectroscopic stack plot of a CDCl<sub>3</sub>-DMSO-*d*<sub>6</sub> (10:1, v/v) solution of **5b** ( $4.0 \times 10^{-3}$  M) upon addition of TBAF in CD<sub>3</sub>CN. ( $K_a = 477 \pm 14$  M<sup>-1</sup>) and the screen capture from the **1:1** global fit analysis using <http://supramolecular.org>.



| 5a (mol <sup>-1</sup> ) | F <sup>-</sup> (mol <sup>-1</sup> ) | NH <sub>a</sub> Proton (ppm) | NH <sub>b</sub> Proton (ppm) |
|-------------------------|-------------------------------------|------------------------------|------------------------------|
| 4.00E-03                | 0                                   | 7.720                        | 7.150                        |
| 4.00E-03                | 2.00E-03                            | 8.800                        | 7.550                        |
| 4.00E-03                | 4.00E-03                            | 9.700                        | 7.900                        |
| 4.00E-03                | 8.00E-03                            | 10.500                       | 8.640                        |
| 4.00E-03                | 1.20E-02                            | 11.000                       | 8.980                        |
| 4.00E-03                | 1.60E-02                            | 11.250                       | 9.340                        |
| 4.00E-03                | 2.00E-02                            | 11.400                       | 9.440                        |

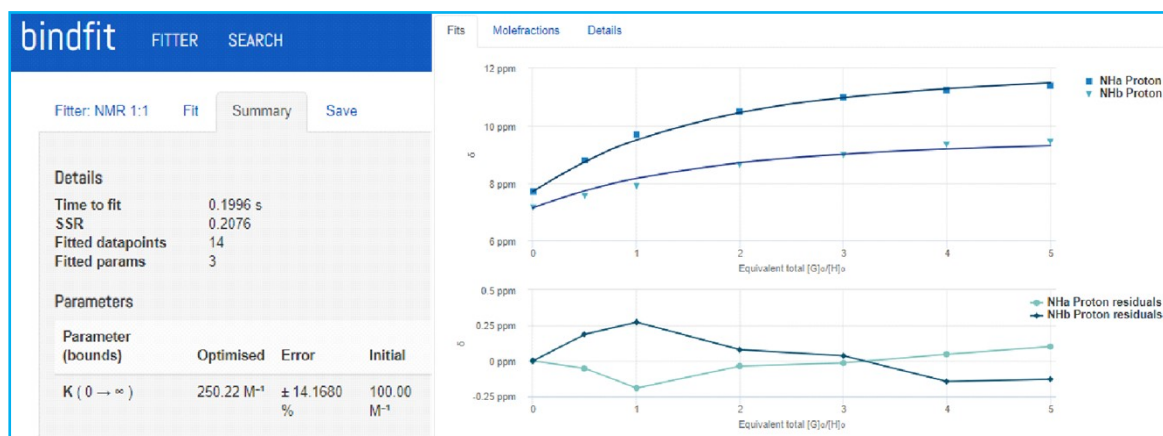


**Figure S19.** <sup>1</sup>H NMR spectroscopic stack plot of a CDCl<sub>3</sub>-DMSO-*d*<sub>6</sub> (10:1, v/v) solution of **5a** ( $4.0 \times 10^{-3}$  M) upon addition of TBAF in CD<sub>3</sub>CN. ( $K_a = 250 \pm 14$  M<sup>-1</sup>), and the screen capture from the **1:1** global fit analysis using <http://supramolecular.org>.

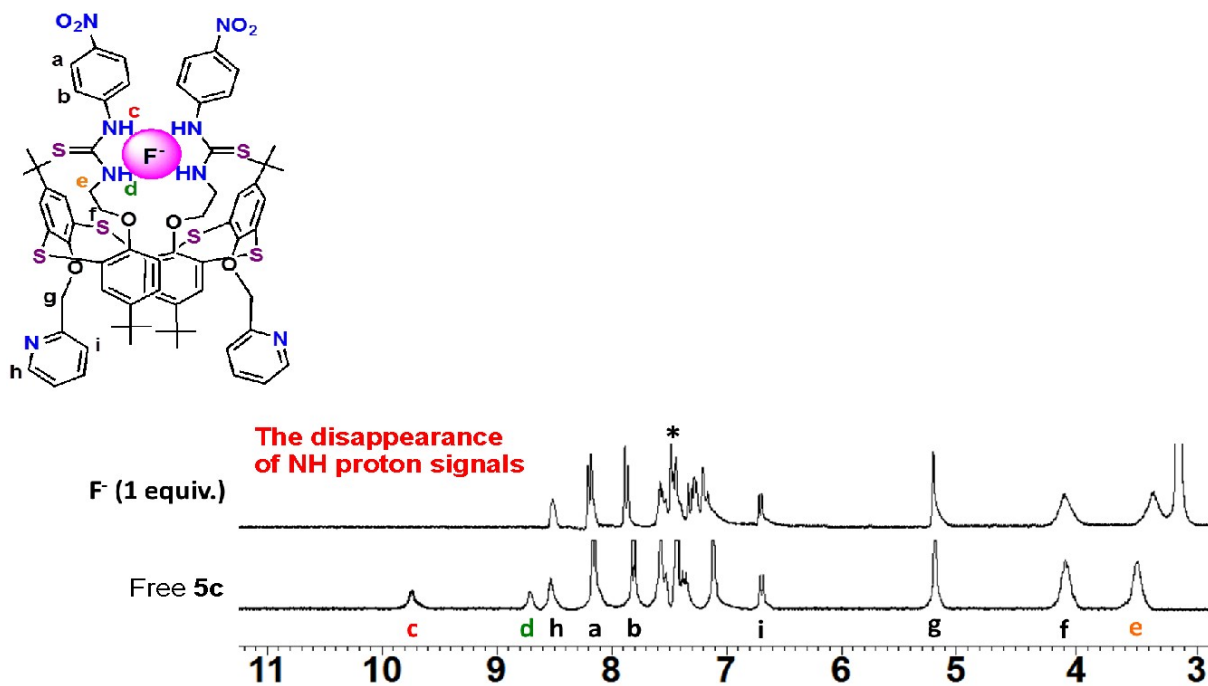


**Figure S20.** <sup>1</sup>H NMR spectroscopic stack plot of a CDCl<sub>3</sub>–DMSO-*d*<sub>6</sub> (10:1, v/v) solution of **5c** ( $4.0 \times 10^{-3}$  M) upon addition of TBAF in CD<sub>3</sub>CN.

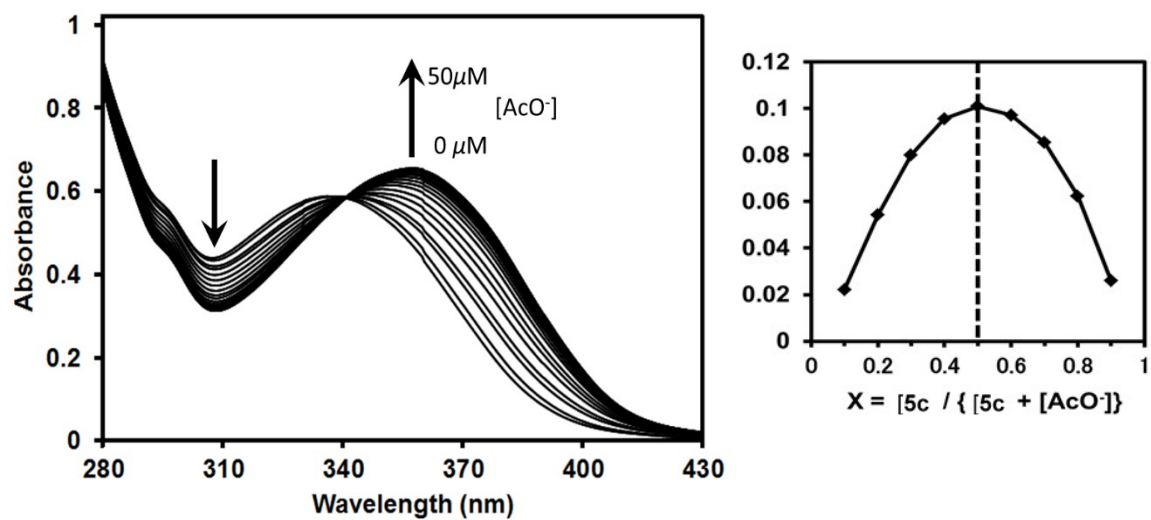


**Figure S21.** *Left:* UV–vis absorption spectra changes of **5c** (2.5 μM) upon the addition of AcO<sup>-</sup> ion (0–50 μM) as its tetrabutylammonium salt in CH<sub>2</sub>Cl<sub>2</sub>–DMSO (10:1, v/v) at 298 K. *Right:* Job plot showing the 1:1 binding of **5c** to AcO<sup>-</sup> ion from the UV-vis titration method at 358 nm in CH<sub>2</sub>Cl<sub>2</sub>–DMSO (10:1, v/v).

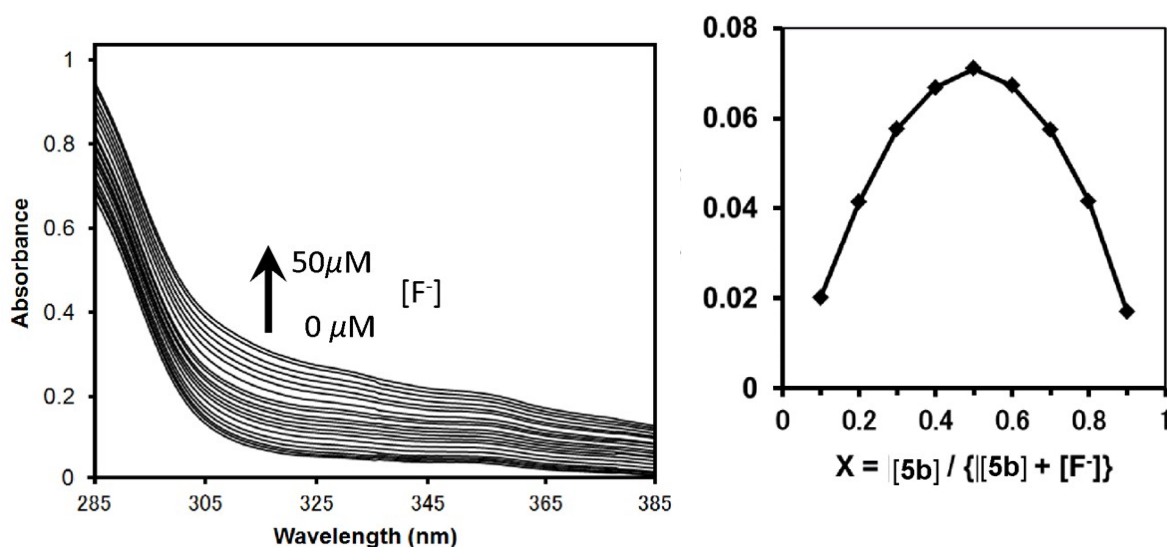


**Figure S22.** *Left:* UV-vis absorption spectra changes of **5b** (2.5  $\mu\text{M}$ ) upon the addition of  $\text{F}^-$  ion (0–50  $\mu\text{M}$ ) at 298 K as a TBAF salt in  $\text{CH}_2\text{Cl}_2$ –DMSO (10:1, v/v). *Right:* Job's plot showing the 1:1 binding of **5b** to  $\text{F}^-$  ion from the UV-vis titration method at 358 nm in  $\text{CH}_2\text{Cl}_2$ –DMSO (10:1, v/v).

**Table S1.** The DFT interaction energies  $\Delta\text{IE}$  ( $\text{kJ mol}^{-1}$ ) calculated from the geometry optimized structure of receptors **L** (For: **5a**: R= H; **5b**: R= F; and **5c**: R=  $\text{NO}_2$ ) and complexes with the anions ( $\text{F}^-$ ,  $\text{Cl}^-$ ,  $\text{AcO}^-$ , and  $\text{H}_2\text{PO}_4^-$ ) and cation  $\text{Ag}^+$  using B3LYP/LANL2DZ basis set in gas phase, dichloromethane (DCM) and dimethyl sulfoxide (DMSO) solvent system using *Gaussian 16*<sup>1</sup> at the B3LYP level of DFT and the LANL2DZ basis set.<sup>2</sup>

| Complex  | $\Delta\text{IE}$ ( $\text{kJ mol}^{-1}$ ) in gas phase |                     |                                  | $\Delta\text{IE}$ ( $\text{kJ mol}^{-1}$ ) in DCM solvent |                     |                                  | $\Delta\text{IE}$ ( $\text{kJ mol}^{-1}$ ) in DMSO solvent |                     |                                  |
|--|---|---------------------|----------------------------------|---|---------------------|----------------------------------|--|---------------------|----------------------------------|
|  | <b>5a</b><br>(R= H)                                     | <b>5b</b><br>(R= F) | <b>5c</b><br>(R= $\text{NO}_2$ ) | <b>5a</b><br>(R= H)                                       | <b>5b</b><br>(R= F) | <b>5c</b><br>(R= $\text{NO}_2$ ) | <b>5a</b><br>(R= H)  | <b>5b</b><br>(R= F) | <b>5c</b><br>(R= $\text{NO}_2$ ) |
| <b>L</b> $\supset$ $\text{F}^-$                | -484.91   | -505.38             | -551.35                          | -242.11   | -249.53             | -274.69                          | -206.34  | -225.79             | -231.55                          |
| <b>L</b> $\supset$ $\text{Cl}^-$               | -296.45   | -317.00             | -362.33                          | -112.51   | -118.86             | -138.44                          | -82.87   | -101.32             | -100.61                          |
| <b>L</b> $\supset$ $\text{AcO}^-$              | -294.52   | -314.05             | -361.34                          | -125.67   | -132.34             | -155.99                          | -95.96   | -115.25             | -104.33                          |
| <b>L</b> $\supset$ $\text{H}_2\text{PO}_4^-$   | -268.66   | -289.58             | -339.47                          | -119.77   | -126.41             | -136.37                          | -91.63   | -105.16             | -101.83                          |
| <b>L</b> $\supset$ $\text{Ag}^+$               | -440.17   | -436.59             | -436.38                          | –   | –                   | –                                | v  | –                   | –                                |
| <b>L</b> $\supset$ $\text{Ag}^+$               | –   | -435.64             | –                                | –   | -169.28             | –                                | –  | -146.90             | –                                |
| $\text{Ag}^+$ <b>cL</b> $\supset$ $\text{F}^-$ | –   | -1090.11            | –                                | v   | -417.73             | –                                | v  | -364.91             | –                                |

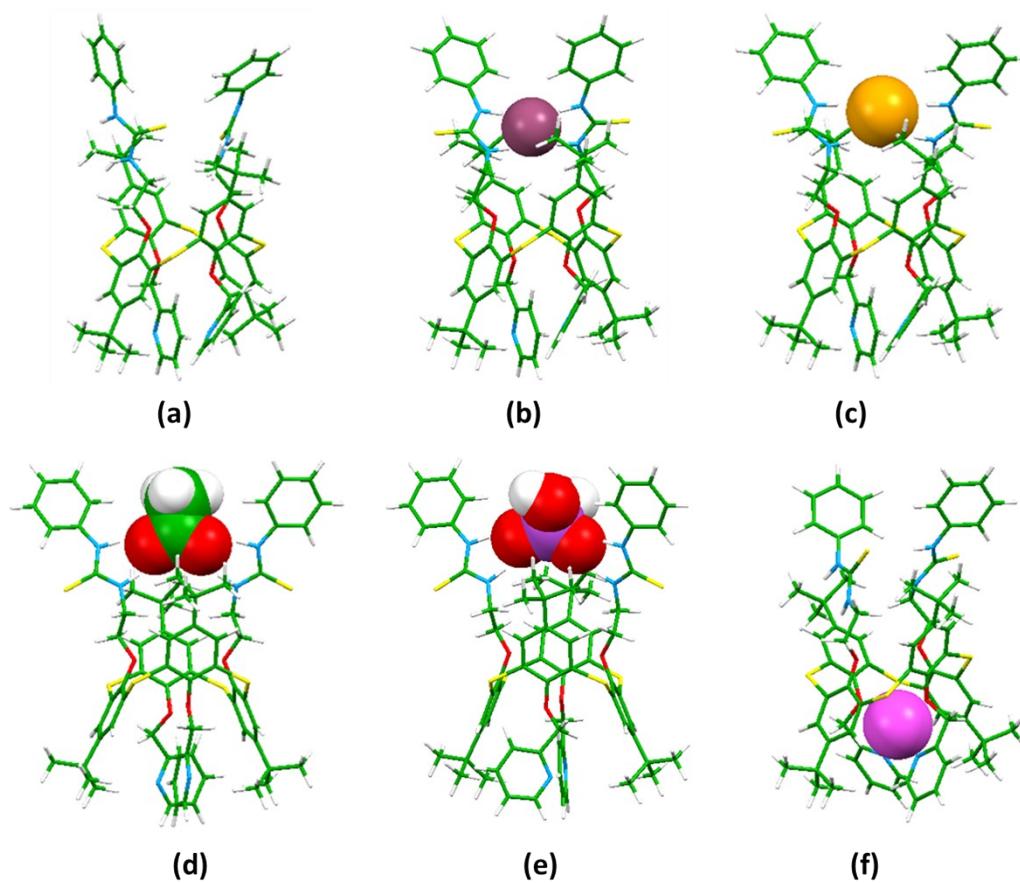


**Figure S23.** Geometry-optimized (PBE0/LANL2DZ) structures of receptor **5a** (R= H) and complexes with the anions (b-e) ( $\text{F}^-$ ,  $\text{Cl}^-$ ,  $\text{AcO}^-$ , and  $\text{H}_2\text{PO}_4^-$ ) and  $\text{Ag}^+$ (f) ion by using B3LYP/LANL2DZ basis set in gas phase. Colour code: carbon atoms = green, oxygen atoms = red, nitrogen atoms = blue, and  $\text{Ag}^+$  = magenta.  $\text{F}^-$  = purple;  $\text{Cl}^-$  = orange; Hydrogen atoms = white; phosphorus atom= light purple.



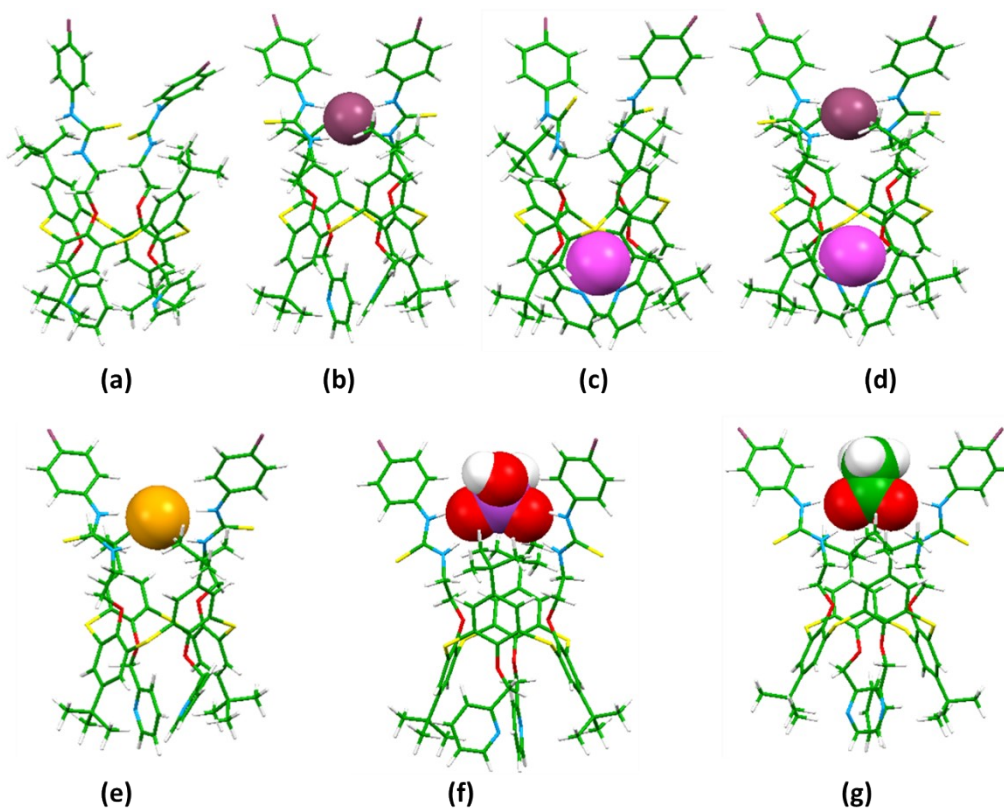


**Figure S24.** Geometry-optimized (PBE0/LANL2DZ) structures of receptor **5b** (R= F) and complexes with the anions ( $F^-$ ,  $Cl^-$ ,  $AcO^-$ , and  $H_2PO_4^-$ ),  $Ag^+$  ion (c) and  $Cl^-$  in presence of  $Ag^+$  ion (d) by using B3LYP/LANL2DZ basis set in gas phase. Colour code: carbon atoms = green, oxygen atoms = red, nitrogen atoms = blue, and  $Ag^+$  = magenta.  $F^-$  = purple;  $Cl^-$  = orange; Hydrogen atoms = white; phosphorus atom = light purple.

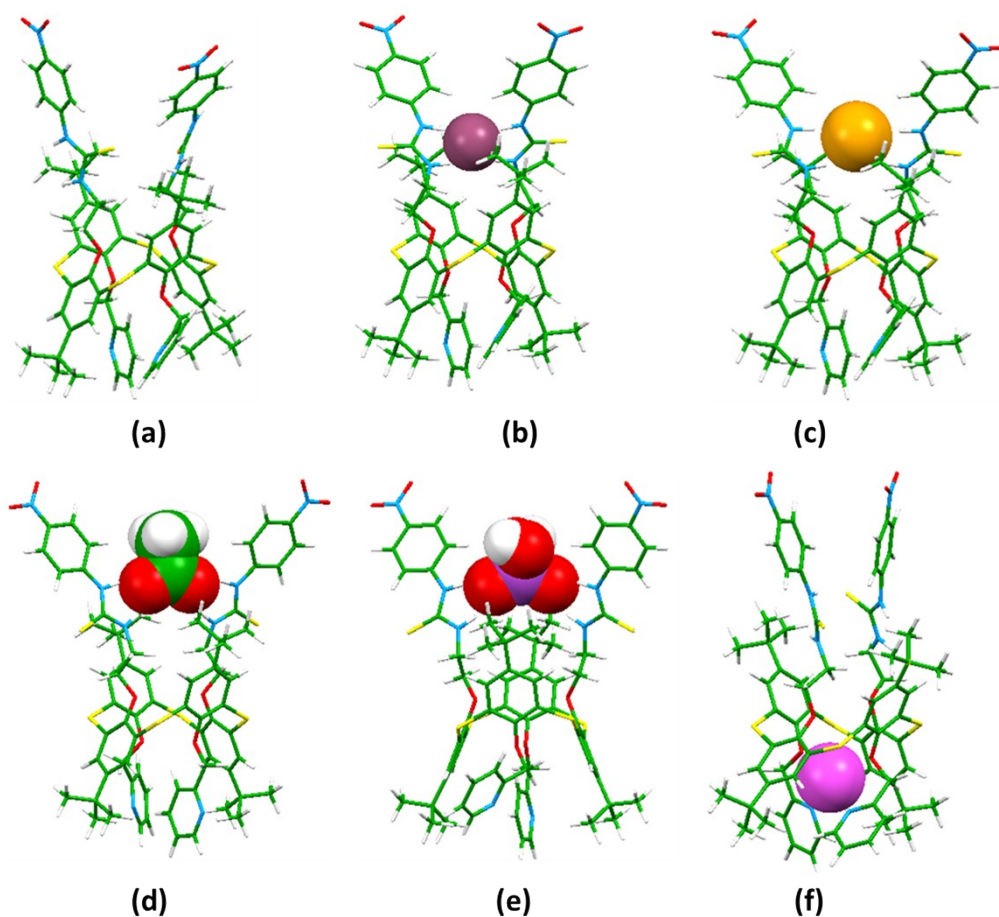


**Figure S25.** Geometry-optimized (PBE0/LANL2DZ) structures of receptor **5c** ( $R = \text{NO}_2$ ) and complexes with the anions ( $\text{F}^-$ ,  $\text{Cl}^-$ ,  $\text{AcO}^-$ , and  $\text{H}_2\text{PO}_4^-$ ) and  $\text{Ag}^+$  ion by using B3LYP/LANL2DZ basis set in gas phase. Colour code: carbon atoms = green, oxygen atoms = red, nitrogen atoms = blue, and  $\text{Ag}^+$  = magenta.  $\text{F}^-$  = purple;  $\text{Cl}^-$  = orange; Hydrogen atoms = white; phosphorus atom = light purple.

**References:**

1. M. J. Frisch, *et al.*, *Gaussian 16*, Revision C.01 Gaussian, Inc., Wallingford CT, 2019.
2. (a) J. P. Perdew, K. Burke, M. Ernzerhof, Generalized Gradient Approximation Made Simple. *Phys. Rev. Lett.* 1996, **77**, 3865; (b) J. P. Perdew, K. Burke, M. Ernzerhof, Generalized Gradient Approximation Made Simple. *Phys. Rev. Lett.* 1997, **78**, 1396.